Interannual and Interdecadal Variability of Winter Precipitation over China in Relation to Global Sea Level Pressure Anomalies

Jianjun Xu[①②] and Johnny C. L. Chan

Department of Physics & Materials Science, City University of Hong Kong

(Received October 8, 2001; revised July 8, 2002)

ABSTRACT

Based on the method of rotated principal component (RPC) analysis and wavelet transforms, the winter precipitation from 36 stations over China for the period 1881–1993 is examined. The results show that the three leading space–time modes correspond, in sequence, to winter rainfall anomalies over the reaches of the Yangtze River, the bend of the Yellow River, and the northeastern region of China. The three modes exhibit interannual oscillations with quasi–biennial and 8–year periods as well as interdecadal oscillations with 16– and 32–year periods. The interannual oscillation (< 10 years) occurs in phase over the different areas, and its maximum amplitude migrates northward considerably with prominent interdecadal variations. However, the interdecadal oscillations (10–32 years) are out of phase over the different regions, and the amplitude variations have the characteristics of stationary waves.

The rainfall anomalies appear to be closely related to the anti–phase changes of mean sea–level pressure (SLP) over the Asian mainland and the North Pacific. When the SLP rises over the North Pacific and decreases over the Asian mainland, the precipitation over East China increases noticeably. The linkage between the rainfall over China and the SLP anomalies apparently results from the strength of the East Asian winter monsoon and its associated temperature and moisture advection.

Key words: wavelet transform, winter precipitation, China, SLP

1. Introduction

Recent analysis of observations and results from general circulation models (GCMs) has revealed interdecadal climate variabilities in a number of meteorological and oceanographic elements. For example, the sea surface temperature (SST) in the central and eastern tropical Pacific has increased significantly since the mid 1970s (Nitta and Yamata 1989; Kumur et al. 1994; Wang 1995; Latif and Barnett 1996). Trenberth (1990) also showed a significant change in the sea–level pressure over the North Pacific in the mid 1970s. A general conclusion is that the interdecadal variability in the Northern Hemisphere (NH) meteorological conditions follows from that of SST over the central eastern tropical Pacific, and the impact is realized mainly through the Pacific–North American (PNA) pattern (Wallace 1993; Trenberth and Hurrell 1994; Graham 1994; Lau and Nath 1996). However, the physical cause of

①Corresponding author address: Dr. Jianjun Xu, Department of Earth & Environmental Science, New Mexico Tech, 801 Leroy Place, Socorro, New Mexico, 87801, USA.

②E–mail: xujj@nmt.edu

the interdecadal variability is not yet clearly understood.

The climate of China is largely influenced by the East Asian monsoon, which is an important and active component in the global climate system, especially in the tropical atmospheric and oceanic interaction system (Yasunari 1990; Lau 1992). Therefore, studies on the climate variability in China can contribute toward a better understanding of the variability of the global oceanic–atmospheric system. Recent observational studies have shown a significant interdecadal variability in the intensity of the East Asian winter monsoon (EAWM) during the past century (Xu and Chan 2001), which is found to be closely related to El Niño events. However, few investigations have been made on the interdecadal variability of winter precipitation in China and its association with the general circulation in the NH, which is the main focus of the present study. A tentative mechanism of the interannual and interdecadal variation of winter precipitation in China is also proposed.

In section 2, the datasets and methodologies used are described. Section 3 documents in detail the interannual and interdecadal variabilities of winter precipitation over China. The possible relationship between the winter precipitation and the sea level pressure over the north Pacific are explored in section 4. All the results are then summarized in section 5.

2. Datasets and methodology

2.1 *Datasets*

The data used are drawn from a number of sources. Monthly winter (December – February) mean precipitation and temperature data of 36 stations in China from 1881 through 1993 are from the compilation by the Nanjing Institute of Meteorology. Missing values are

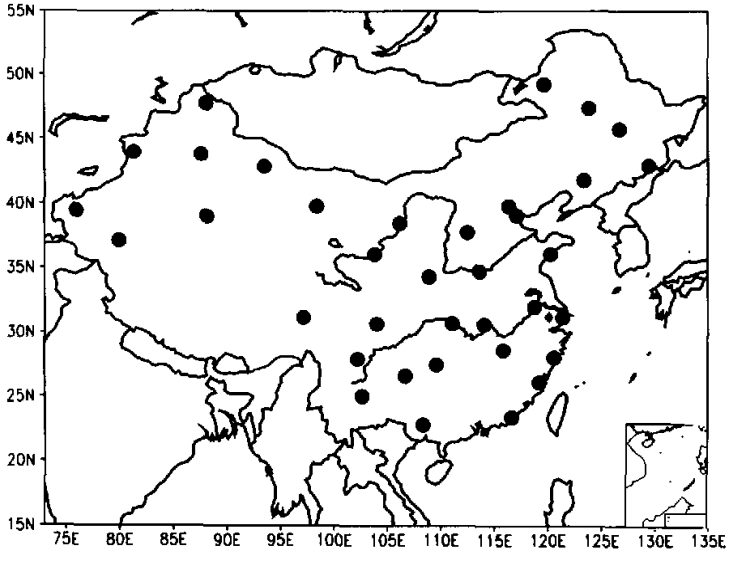

Fig. 1. Location of rainfall stations used in this study.

interpolated from the neighboring observational stations (Shi and Zhu 1996). The geographical distribution of the stations is generally uniform, especially in the eastern part of China (Fig. 1). Note that the reasonability of precipitation data before the1950s needs to be verified further in future work. Monthly NH mean sea-level pressure (SLP) data on a resolution of 5° latitude × 10° longitude during 1873–1993 are from the UK Meteorological Office.

2.2 *Methodology*

The methods of rotated principal component (RPC) analysis and wavelet transforms (WT) are used. The RPC analysis technique was described by Richman (1981). Based on randomly-generated synthetic datasets, he found that the rotated solutions were statistically more robust than their unrotated counterparts, which is consistent with the previous experience of Horel and Wallace (1981).

Unlike the Fourier transform, the wavelet transform decomposes a time series into components in frequency–time space. It can describe the instantaneous phase and amplitude of a component at a specific frequency during its evolution (Meyers et al. 1993). This feature gives it the capability to identify the temporal behavior of particular variation components and to "visualize" the development of these variations including their association with the other variation components. In the transformed frequency–time space, the relative significance of a component to the total variance is defined by its amplitude. In the present analysis, the Morlet function is used as the mother wavelet.

3. The interannual and interdecadal variability of winter rainfall in China

The first spatial mode of the winter precipitation obtained from the RPC method accounts for 11% of the total variance, with the strongest anomalies in the mid and lower reaches of the Yangtze River (Fig. 2). The variance contribution of the second mode is 7.84%, with its maximum over the bend of the Yellow River. The third mode, which explains 7.79% of the variance, shows the anomalies to be mainly in the northeastern part of China.

The time series of the first RPC mode (Fig. 3a) shows that the precipitation anomalies over the mid and lower reaches of the Yangtze River display strong interannual and interdecadal variations. Abundant precipitation existed in 1905, 1936, 1947, 1953, and 1989, and dry conditions occurred in 1903, 1907, 1917, 1933, 1962, 1967, and 1985. Significant interdecadal variations also exist. To identify the multiple time scale variation of winter precipitation anomalies, the wavelet transform method is used to obtain all possible oscillations and then to reconstruct two components using a threshold of 10 years to obtain the interannual (< 10 years) and interdecadal oscillations (> 10 and < 32 years). The frequency–time section (Fig. 3b) and the reconstructed interannual and interdecadal variations (Fig. 3c) show that the precipitation anomalies display the following oscillations: quasi-biennial (QBO), 8-year, with the amplitude of the 4- and 16-year oscillations being smaller.

The amplitude and period of the interannual oscillations also show noticeable interdecadal variations. For example, the QBO was very strong during the period of 1930–1940, the 1950s, and the 1970s, but weak at other times. The 8-year oscillation dominated prior to the 1950s and the 4-year oscillation prevailed during the period of 1950–1960. The period of the interannual oscillation increased gradually from 4 to 8 years after 1970. The interdecadal oscillation of rainfall has a considerable quasi 16-year period, with a peak during 1930–1940, and minima in the 1970s and in the beginning of this century (Fig. 3b).

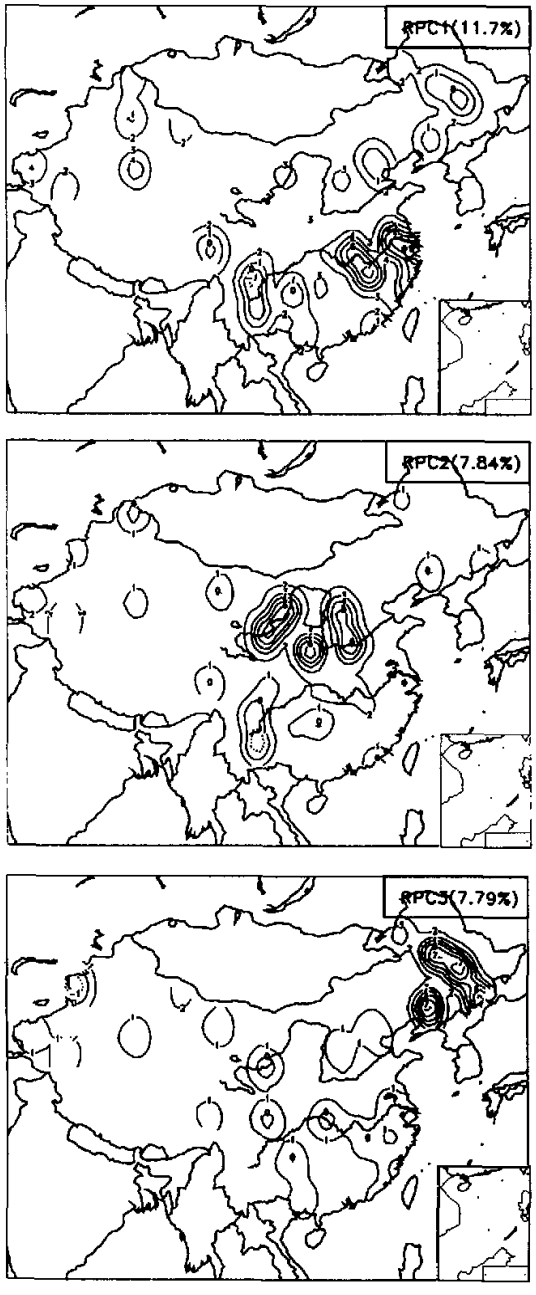

Fig. 2. Spatial distribution of the three leading RPC modes for winter precipitation over China for the period 1881–1993. Shaded areas indicate values >3.0.

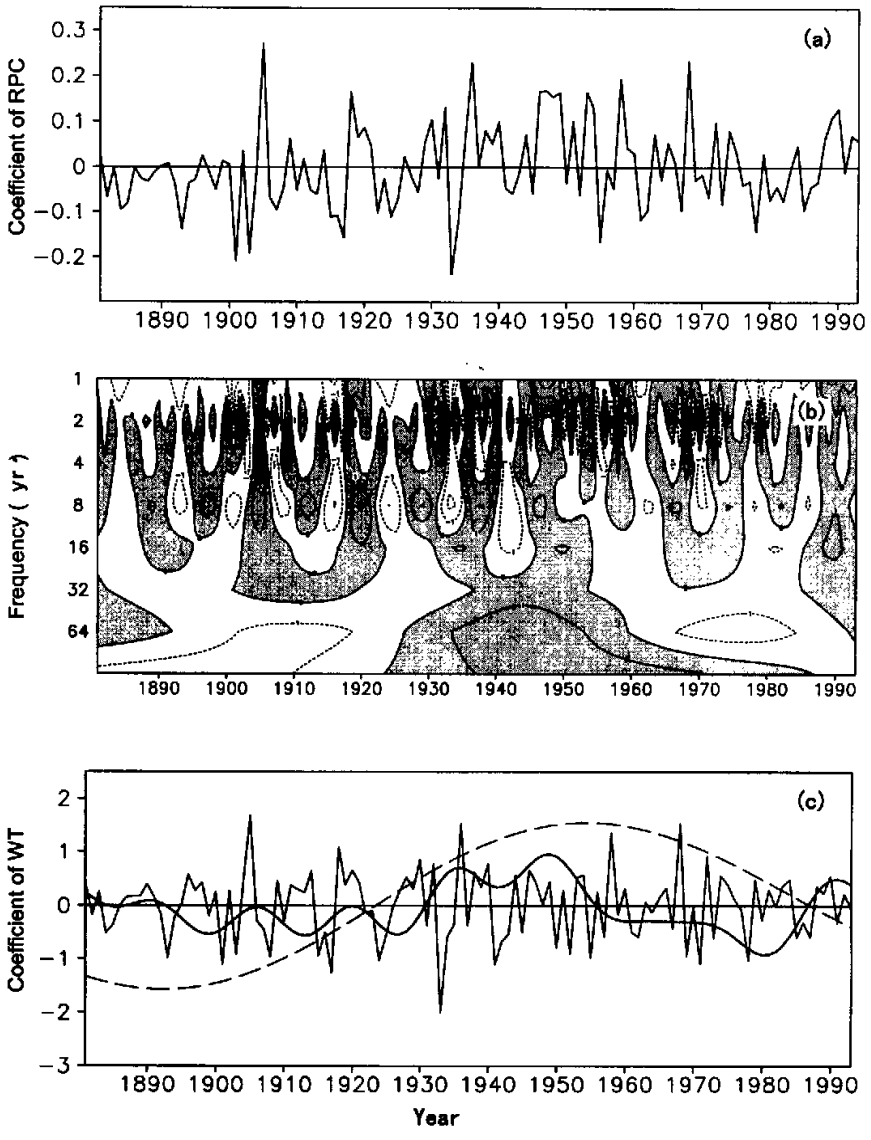

Fig. 3. (a) The time coefficient of RPC1, (b) Real part of the wavelet transform for the RPC1. The shaded areas indicate positive values, (c) Reconstructed interannual component (< 10 years with solid thin line), and the interdecadal component (> 10 and < 32 years with solid thick line) from the wavelet transform (WT), the trend (> 64 years) is indicated by the dashed line.

The trend (period >64 years) decreases on a centennial time scale (dashed line in Fig. 3c). Further, the increases in rainfall in the 1920s and the decreases in the 1970s are also consistent with changes in the global climate (Trenberth 1990; Graham 1994), namely that the global

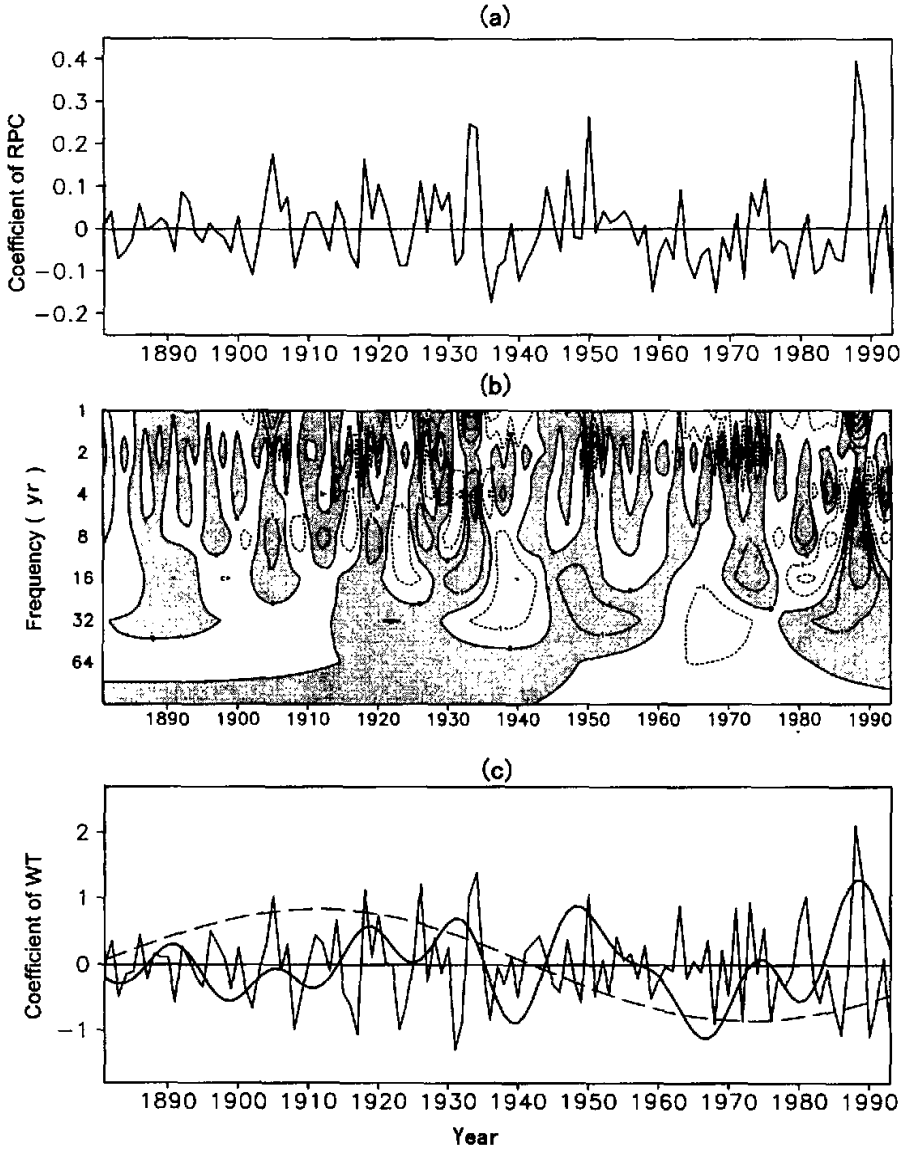

Fig. 4. As in Fig.3 except for the second mode (RPC2).

temperature displayed abrupt changes in the 1920s, and the air–sea interactive systems over the North Pacific showed appreciable interdecadal variations in the 1970s. The relationship between global climate change and rainfall anomalies over China will be discussed in more detail in section 5.

Compared with the first mode, the second RPC mode (Fig. 4) shows that the interannual

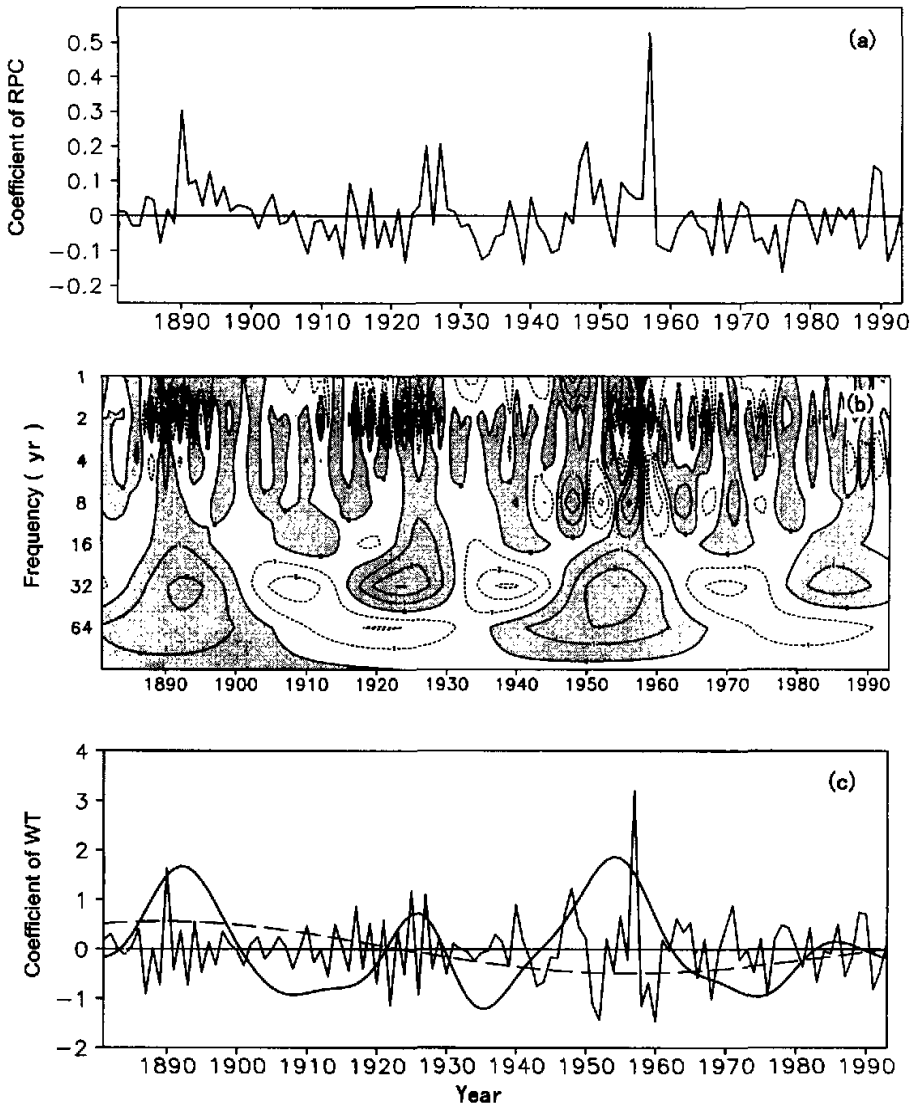

Fig. 5. As in Fig.3 except for the third mode (RPC3).

and interdecadal oscillations in the bend of the Yellow River occur in-phase at times to produce extreme anomalies, such as the positive anomalies in 1905, 1988, and 1989 or the negative anomaly in 1936. The interdecadal oscillations apparently dominate the rainfall variations, and the amplitude of the interannual oscillation is generally weaker than that in the first RPC mode. These results suggest that the rainfall over the bend of the Yellow River will

probably decrease in the next 10 years in terms of the interdecadal variations. On the other hand, according to the centennial time scale, the rainfall would not be less than that in the 1940s and 1960s, both periods being the driest in this century.

The third RPC mode (Fig. 5) shows a very prominent interdecadal oscillation with a 32-year period in the northeast region of China, which is much larger than the interannual variation. The amplitude of the interannual oscillations displays a noticeable interdecadal variability. For example, the QBO was very strong in the 1920s and 1950s, while the 8-year oscillation was dominant during the period 1950–1960.

To identify possible linkages of rainfall anomalies in different areas over the eastern region of China, the rainfall data over the domain (105°–125°E, 20°–50°N) is averaged at 2.5° intervals of latitude to generate 13 time series, each of which is then passed through the wavelet transform. The latitude–time section of the reconstructed series with periods < 10 years shows that the interannual oscillations are in phase from south to north (Fig. 6a). However, the location of maximum amplitude shifts from south to north with an appreciable interdecadal variation. For example, the maximum amplitude occurred in the south (22.5°–30°N) during the period of 1880–1910, then in the middle region (32.5°–40°N) prior to the 1930s but became very weak in the 1940s. From the 1950s, two preferred centers of maxima appeared one over the high latitude domain (40°–45°N) and one over the southern areas (~25°N).

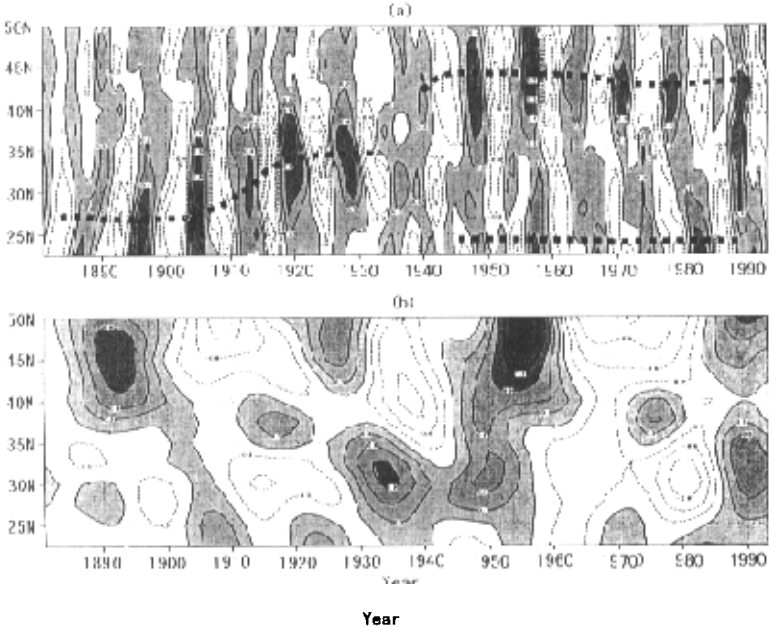

Fig. 6. Latitude–time section of the amplitude of the reconstructed components at each 2.5° latitude band over eastern China (105°–125°E) for (a) the interannual oscillation (< 10 years), and (b) the interdecadal oscillation (> 10 and < 32 years). The shaded areas indicate positive values. Thick dashed line shows the location of the oscillation centers.

In contrast, the interdecadal oscillation (Fig. 6b) shows noticeable latitudinal variations. First, the phases of these oscillations are different between the southern and northern areas of China, but with no regular phase propagation. This perhaps reflects the fact that the oscillation period is different in each region. For example, the northern region is dominated by a 32–year oscillation, but the 16–year oscillations are more prominent in the middle area. Second, the locations of maximum amplitude display a stationary wave characteristic, with the two strongest centers located in the 453°–50°N and 27.5°–32.5°N bands. Finally, the interdecadal oscillation in the northern part of China is much stronger than in the southern area.

To summarize, the winter precipitation of China displays interannual and interdecadal oscillations, whose periods increase with latitude, with the northeast region dominated by a 32–year oscillation. The interannual variation of precipitation can be modulated significantly by the interdecadal oscillation. Extreme anomalies occur when the interannual and interdecadal oscillations are in phase.

4. Possible relationship with the sea–level pressure over the Asian–Pacific areas

Winter precipitation in East China is largely controlled by the Asian winter monsoon, which is closely related to the sea–level pressure (SLP) contrast between the Asian landmass and the North Pacific (Shi and Zhu 1996; Xu et al. 1997a, b). The possible mechanism for the winter precipitation anomalies in China will be discussed in this section from this perspective.

Similar to the method in section 4, the SLP data are decomposed into the two oscillation components (interannual and interdecadal). The correlation between the time series of the three precipitation RPC modes and SLP on the interannual basis indicates that the rainfall variations over the reaches of the Yangtze River and the northeastern region of China are closely related to those in the SLP (Figs. 7a, b). No significant relation, however, exists for the rainfall over the bend of Yellow River (not shown). The rainfall anomalies over the reaches of the Yangtze River show a positive correlation with SLP over the subtropical north-central Pacific and off the northeast coast of China, and a negative one over the southeastern region of China (Fig. 7a). Such a distribution of pressure anomalies suggests a southeasterly, low–level airflow going into central East China, which tends to bring warm and moist air into the region. This would likely cause more precipitation in that area. The pressure anomalies in Fig. 7b imply a weaker Siberian anticyclone, which is consistent with a weaker Aleutian low. With such a configuration, flow anomalies over northeastern China where the RPC3 mode has a maximum (see Fig. 2) are likely to be southeasterly from over the ocean and westerly or southwesterly from the west. These anomalies would again facilitate the development of above–normal precipitation in the region.

On interdecadal time scales, the pressure anomalies correlate with all three RPC modes (Fig. 8). The three correlation patterns imply essentially the same features, i.e., for positive precipitation anomalies to occur in each of the regions, positive SLP anomalies should exist over the North Pacific and negative anomalies over the Asian mainland. However, some differences in each of the correlation maps are also apparent. For both the Yangtze River region and northeastern China (Figs. 8a and c), the increase in precipitation is mainly due to a weakening of the Mongolian high. Further more, the negative SLP anomalies over the Yangtze River (Fig. 8a) imply persistent frontal activity there, which would likely bring more precipitation. The large area of negative SLP anomalies over the Asia mainland associated with RPC3 (Fig. 8c) suggests above–normal southwesterlies coming into northeastern China, and

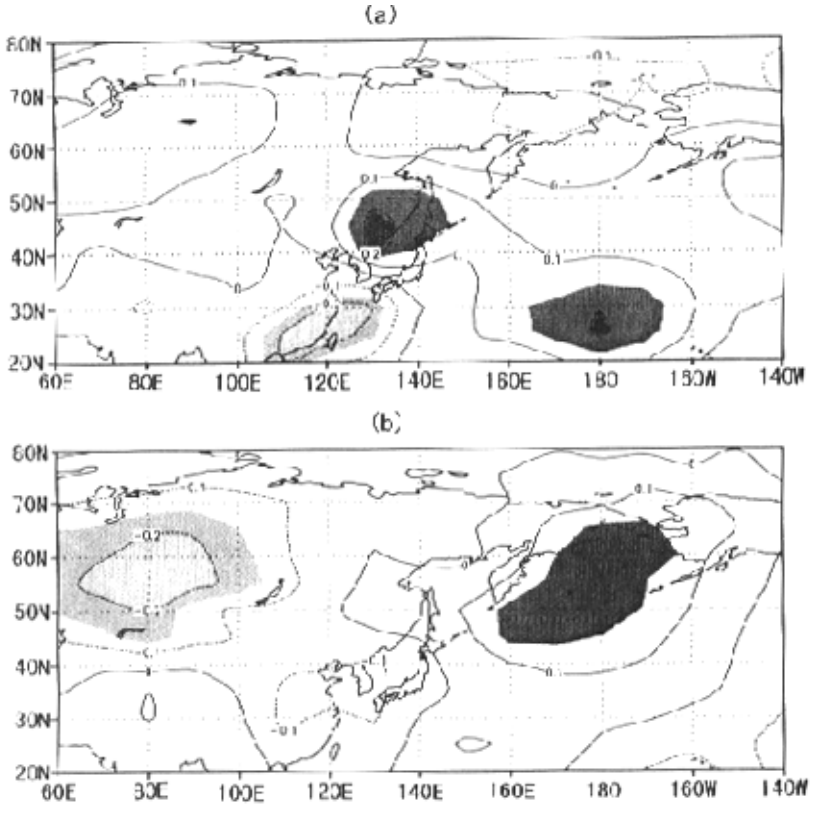

Fig. 7. Correlation between winter mean sea-level pressure (SLP) and the time series of the two leading mode on the interannual basis (< 10 year).(a) RPC1, (b) RPC3. The figure correlated with RPC2 isn't shown, the shaded area exceeds 0.05 level of significance.

hence giving a higher chance of above-normal precipitation. For the bend of the Yellow River (Fig. 8b), the pattern of the correlation shows a bigger difference from both the Yangtze River (Fig. 8a) and Northeastern China (Fig. 8c). The positive SLP anomalies extend from the Northwest Pacific into the Asian mainland, which apparently benefits the east-west transportation of moist air from the ocean to the mainland.

The results suggest that the interannual and interdecadal oscillations of winter precipitation over China have a close relationship with pressure oscillations over the North Pacific and Asian mainland. Climatologically, the winter SLP pattern consists of the Mongolian/Siberian high over the Asian mainland and the Aleutian low over the North Pacific. This zonal pressure gradient is of course closely related to the land-sea thermal contrast. Many studies (e.g., Shi and Zhu 1996; Xu et al. 1998) suggest that this gradient determines the variation of the East Asian winter monsoon. The patterns in Figs. 7 and 8 show that the regimes with the highest correlations are generally over the pressure activity centers, which means that the

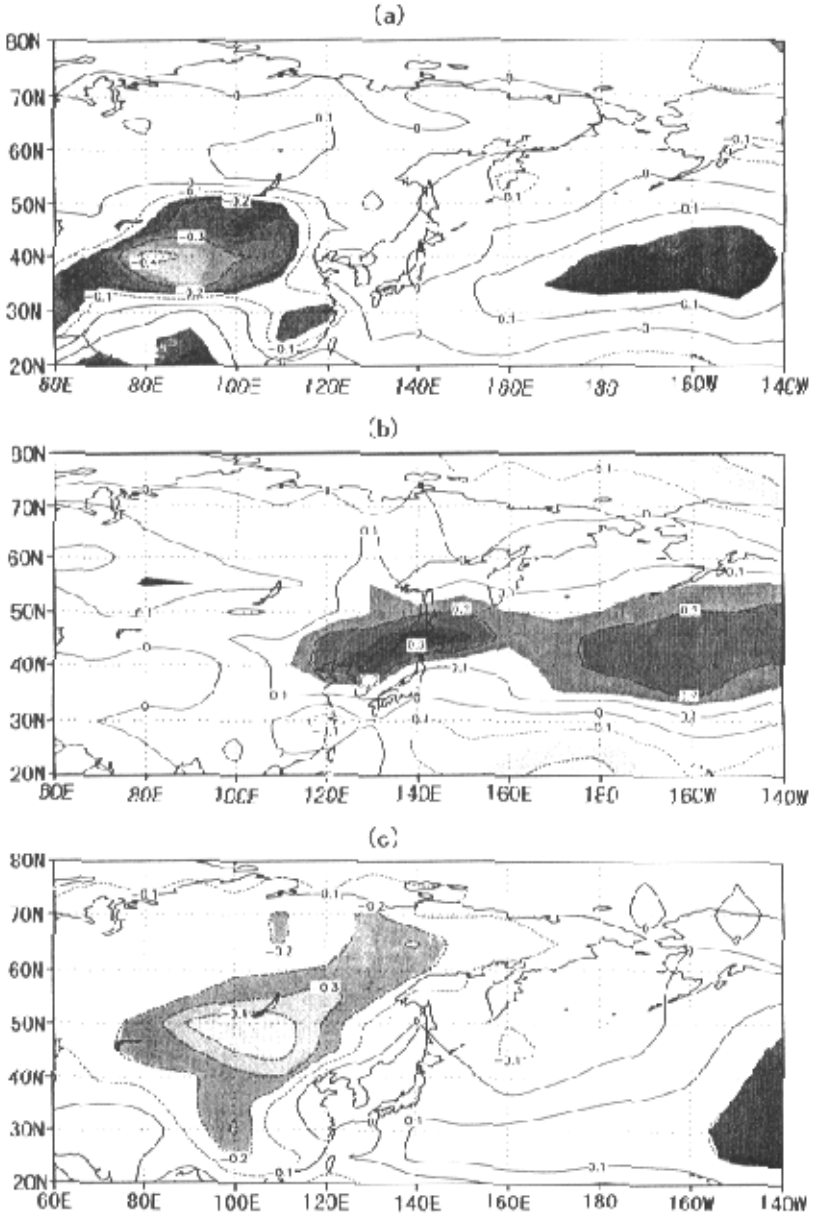

Fig. 8. Correlation between winter mean sea level pressure (not used in text) and the time series of the three leading modes on the interdecadal basis (>10 and <32 years). (a) RPC1, (b) RPC2, (c) RPC3. The shaded area exceeds the 0.05 level of significance.

East Asian winter monsoon anomalies have a significant impact on the winter precipitation over the eastern part of China. A pressure rise in the North Pacific and a decrease over the Asian mainland imply a weak winter monsoon. This leads to weaker northerlies and thus favors a northward transport of warm and moist air, resulting in precipitation increases over the eastern part of China.

5. Summary and discussion

Using the RPC and wavelet transform methods, the interannual and interdecadal variabilities of winter precipitation of 36 stations over China for the period 1881–1993 are studied. The major results can be summarized as follows.

The three leading space–time modes show that the winter precipitation variations mainly occur over the lower reaches of the Yangtze River, the bend of the Yellow River, and the northeastern region of China. The interannual oscillations have quasi–biennial and 8–year periods, while 16– and 32–year oscillations are found on interdecadal time scales. Noticeable differences in each of the regions are also observed.

The interannual oscillation of precipitation is modulated by the interdecadal variation. When both of them are in phase, the precipitation tends towards an extreme anomaly. The interdecadal oscillation predominates in northeastern China while the interannual oscillation is stronger in the southern part of China.

The interannual oscillations at low and high latitudes are in phase, but the maximum amplitude shifts from south to north on interdecadal time scales. On the other hand, the phases of interdecadal oscillations at different latitudes differ, and the maximum amplitude displays the characteristics of a stationary wave.

The interannual and interdecadal variations of precipitation over the eastern part of China correlate well with the pressure anomalies over the Asian mainland and the North Pacific. When pressure rises over the North Pacific and falls over the Asian mainland, the precipitation tends to increase, which is closely related to the East Asian winter monsoon anomalies.

This paper identifies changes in the sea–level pressure over the Asian mainland and the North Pacific as a possible mechanism responsible for the interannual and interdecadal variations in winter precipitation over the eastern parts of China. Such changes of course are related to those in the planetary–scale circulations. Thus, predictions of the interannual variations of winter precipitation in these regions could only be accomplished effectively using general circulation models. Nevertheless, this study shows that it is possible to understand such variations through the variations in the pressure patterns. The next step would be to identify the physical mechanisms responsible for the "oscillations" in these pressure patterns, to be reported in a future paper.

Acknowledgments. The authors would like to thank the Nanjing Institute of Meteorology for providing the precipitation data, and the UK Meteorological Office for providing the mean sea level pressure data. This research is sponsored by the City University of Hong Kong Research Grant Nos. 7100092, 9360017, and 8780046.

REFERENCES

Graham, N. E., 1994: Decadal–scale climate variability in the tropical and North Pacific during the 1970s and 1980s: Observations and model results. *Climate Dyn.*, **10**, 135–162.

Horel, J., and J. Wallace, 1981: Planetary–scale atmospheric phenomena associated with the Southern Oscillation.

Mon. Wea. Rev., **109**, 813–829.

Kumur, A., A. Leetmaa, and M. Ji, 1994: Simulation of atmospheric variability induced by sea surface temperatures and implications for global warming. *Science*, **266**, 632–634.

Latif, M., and T. P. Barnett, 1996: Decadal climate variability over the North Pacific and North America: Dynamics and predictability. *J. Climate*, **9**, 2407–2423.

Lau, K. M., 1992: East Asian summer monsoon rainfall variability and climate teleconnection. *J. Meteor. Soc. Japan*, **70**, 211–242.

Lau, N. C., and M. J. Nath, 1996: The role of the "atmospheric bridge" in linking tropical Pacific ENSO events to extratropical SST anomalies. *J. Climate*, **9**, 2036–2057.

Meyers, S. D., B. G. Kelly, and J. J. O'Brien, 1993: An introduction to wavelet analysis in oceanography and meteorology: With application to the dispersion of Yanai waves. *Mon. Wea. Rev.*, **121**, 2858–2866.

Nitta, T., and S. Yamata, 1989: Recent warming of the tropical sea surface temperature and its relationship to the Northern Hemisphere circulation. *J. Meteor. Soc. Japan*, **67**, 375–383.

Richman, M. B., 1981: Obliquely rotated principal components: An improved meteorological map typing technique. *J. Appl. Meteor.*, **20**, 1145–1159.

Shi, N., and Q. Zhu, 1996: An abrupt change in the intensity of the East Asian summer monsoon index and its relationship with temperature and precipitation over East China. *International Journal of Climatology.*, **16**, 757–764.

Trenberth, K. E., 1990: Recent observed interdecadal climate changes in the Northern Hemisphere. *Bull. Amer. Meteor. Soc.*, **71**, 988–993.

Trenberth, K., and J. W. Hurrell, 1994: Decadal atmosphere–ocean variations in the Pacific. *Climate Dyn.*, **9**, 303–319.

Wallace, J. M., 1993: Structure and seasonality of interannual and interdecadal variability of the geopotential height and temperature fields in the Northern Hemisphere troposphere. *J. Climate*, **6**, 2063–2082.

Wang, B., 1995: Interdecadal changes in El Niño onset in the last four decades. *J. Climate*, **8**, 267–285.

Xu, J. J., Q. Zhu, and N. Shi, 1997a: East–Asian Winter Monsoon–ENSO Cycle Relation with Interdecadal Anomaly in the Past 100 Years. *Chinese Journal of Atmosphereic Sciences*, **4**, 325–331.

Xu, J. J., Q. Zhu, and N. Shi, 1997b: The Singular Spectral Analysis of Periodic Oscillation in long–term Variation of East–Asian Monsoon in Recent Century. *Acta Meteor. Sinica*, **55**, 620–627.

Xu, J. J., Q. Zhu, and Z. Sun, 1998: Interrelation between East–Asian Winter Monsoon and Indian / Pacific SST with the Interdecadal Variation. *Acta Meteor. Sinica*, **12**, 275–287.

Xu, J. J., and J. C. L. Chan, 2001: The role of the Asian–Australian monsoon system in the onset time of El Niño events. *J. Climate*, **14**, 418–433.

Yasunari, T., 1990: Impact of Indian monsoon on the coupled atmosphere / ocean system in the tropical Pacific. *Meteor. Atmos. Phys.*, **44**, 29–41.